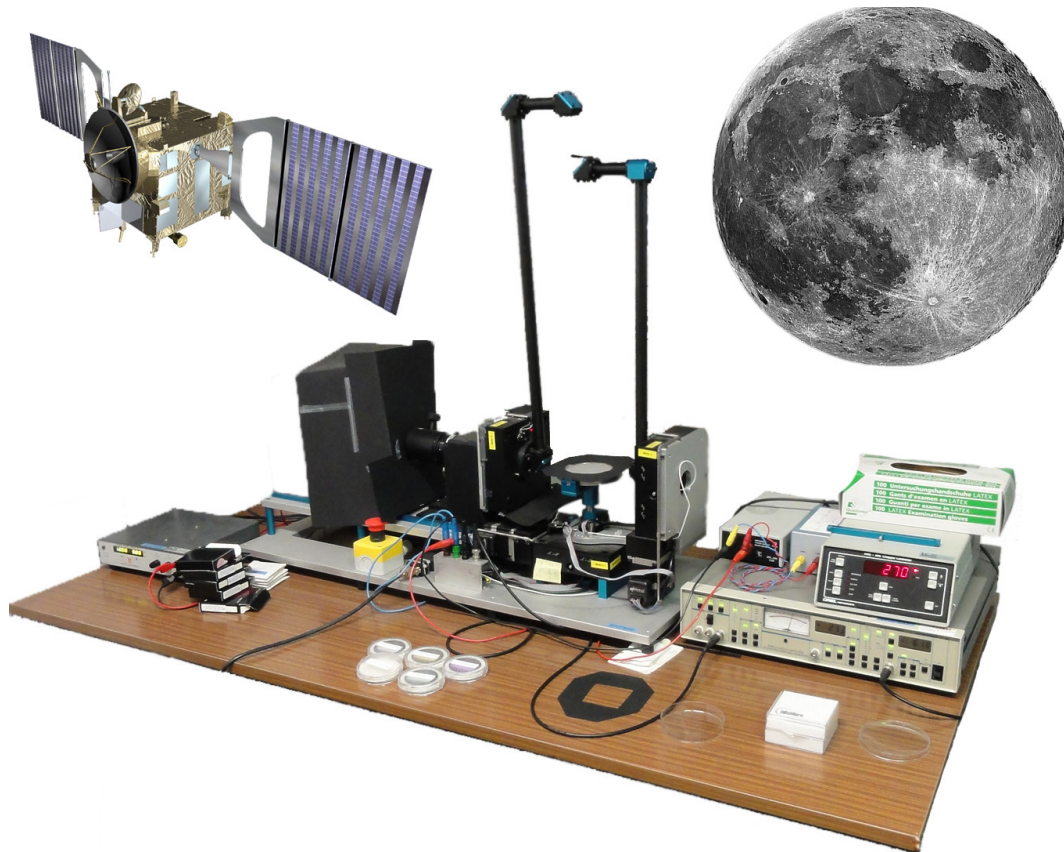


Praktikum für Fortgeschrittene Hauptfachphysiker

Light Scattering



Version 3.2, Oct. 2017:

Antoine Pommerol (antoine.pommerol@space.unibe.ch)

Patricio Becerra (patricio.becerra@space.unibe.ch)

Contents

Objectives:.....	2
1. Introduction:.....	3
2. Definitions:.....	6
3. Physics of the BRDF:	9
4. The PHIRE-1 photo-goniometer:.....	11
5. Exercises:.....	14
References:.....	16
Appendix A (detailed user manual):	17

Objectives:

Use a gonio-radiometer to quantitatively characterize the light scattering behavior of different samples. This practical involves the sample preparation, the use of the gonio-radiometer to acquire measurements, the calibration of the data, and the discussion of the implications of these measurements for various applications.

1. Introduction:

When we observe the surface of an object, by eye or with a camera, we collect some light that is emitted from a source and reflected by the surface of the given object. The apparent brightness of the surface, i.e. the amount of reflected radiance that reaches the eye or the camera, is always dependent on the positions in space of the light source and the observer relative to the surface, as well as the wavelength of the incident light. The bidirectional reflectance distribution function (BRDF) describes the relation between the incident irradiance falling onto the sample and the radiance collected by the detector as a function of the incidence, emission and phase angles. In addition, the spectral BRDF describes the dependence of the BRDF on wavelength. Measuring, modeling and analyzing the BRDF of various types of surfaces is very important in different fields. In particular it is indispensable for remote-sensing of surfaces of the Earth and other Solar System objects.

When acquiring images of planets, moons or small bodies (comets, asteroids, etc.), the sun provides the illumination, and the image is acquired by a sensor on board a spacecraft that may orbit or fly by the observed target. As the observed object rotates and orbits around the sun, and the spacecraft moves above the surface, both the illumination and the observation angles are susceptible to variations. As a result, the apparent brightness (or reflectance) of the surface will also vary. Understanding the relationship between the reflectance and the measurement geometry is crucial for the detailed interpretation of planetary images and can provide valuable information on the physical properties of the surface of study.

As an example, [figure 1](#) shows the relationship between the average reflectance of the Moon and the “phase angle”, i.e., the angle between the illumination and observation directions, obtained from a series of measurements by a camera on-board the lunar orbiter Clementine. This relationship, called the phase function, was derived from low phase angles (when the directions of the sun and the observing spacecraft are close to each other) to phase angles of about 52° , at two different wavelengths: 415 nm (blue)

and 750 nm (red). We see that the apparent brightness of the moon continuously decreases as phase angle increases. There is almost a factor of 4 difference between the reflectance at the lowest phase angles (3°) and that at the highest phase angles (52°), for both wavelengths. This is due to the fact that the incident light flux varies as a function of the cosine of the incidence angle and that the surface of the moon scatters the light anisotropically. The anisotropy of the light scattering originates both from macroscopic (roughness, slopes, shadows...) and microscopic (intrinsic anisotropic scattering by individual grains) scale effects. A direct implication of this phase function is that the full moon observed from Earth (phase angle = 0°) is more than two times brighter than the half moon (phase angle = 90°). In addition, the phase function displays a dependence on wavelength, as relative variations in reflectance are larger in the blue part than in the red part of the spectrum. This means that the apparent color of the Moon is also slightly dependent on measurement geometry.

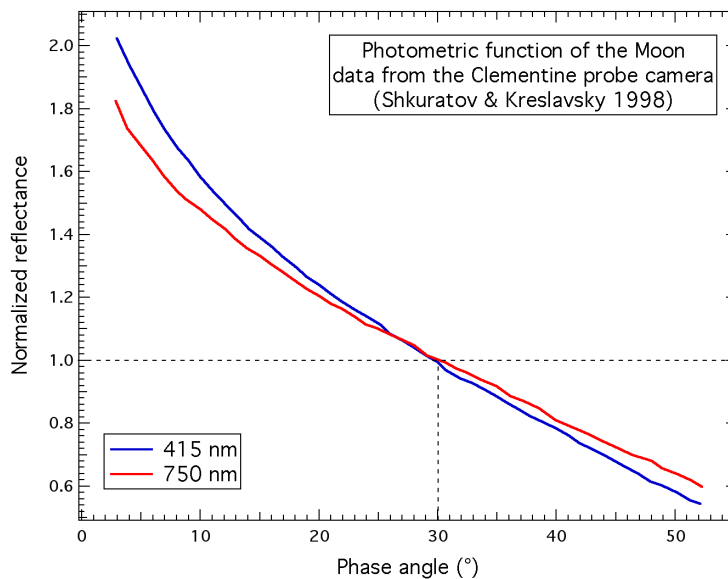


Figure 1: Phase function of the Moon derived at two wavelengths from series of measurements by the Clementine spacecraft camera (data from [Shkuratov and Kreslavski, 1998](#)).

Different physical models have been developed to account for these effects. The most widely used in the planetary remote-sensing community are the ones developed by [Hapke \(2012\)](#) and [Shkuratov et al. \(1999\)](#). They relate the dependence of reflectance on measurement geometry to different physical

parameters of the surface like the size and shape of the grains, the density of the surface or the intrinsic levels of absorption and reflection of light by the surface materials. The inversion of measured photometric data by these models could in theory allow the retrieval of these important parameters. To do this, it is crucial to perform measurements in the laboratory to fully test the models and check their sensitivity to the various parameters. For this reason, instruments called radio-goniometers or photo-goniometers have been developed. The PHIRE-1 (**PH**ysikalisches Institut **R**adiometric **E**xperiment) goniometer that you will use for this practical is one of these instruments. It was developed at Bern University by K. Gunderson and colleagues and is extensively described in [Gunderson et al. \(2006\)](#). Note that in addition to being used for teaching purposes, this instrument has been used for published research to study the light scattering properties of “analog” samples of the surface of the Moon, Mars, and the Saturnian moon Titan ([Gunderson et al., 2006, 2007, 2008](#); [Lüthi, 2009](#)). You are strongly encouraged to have a quick look at these papers to learn more about the scientific rationale, the design and the applications of the PHIRE-1 instrument.

2. Definitions:

So far, we have described the “brightness” or “reflectance” of surfaces and samples in a rather vague way. There are in fact precise physical definitions that must be used to describe how a sample scatters light. However, so many definitions are proposed and used by different authors that the situation is a bit confusing. Here we define the BRDF and the reflectance factor in the simplest way. Use these definitions for your measurements, but don’t be surprised if you find slight variations of these definitions in the literature. Let F [$\text{W}\cdot\text{m}^{-2}$] be the absolute irradiance emitted from the source along the illumination direction. We will describe this direction by the “incidence angle”: θ_i . Let I [$\text{W}\cdot\text{m}^{-2}\cdot\text{sr}^{-1}$] be the absolute radiance measured by the sensor along the emission direction. We will describe this direction by two angles: the “emergence angle”: θ_e and the “azimuth angle”: θ_a . [Figure 2](#) presents the definitions of these angles relative to the observed surface.

The BRDF is then defined as the ratio between radiance scattered from the surface through a solid angle Ω_s [sr] (I) and the irradiance on the sample ($F\cdot\cos(\theta_i)$):

$$BRDF(\theta_i, \theta_e, \theta_a, \lambda) = \frac{I}{F \cdot \cos(\theta_i) \Omega_s} \quad [\text{sr}^{-1}]$$

If the light is scattered by a so-called perfect Lambert surface, the radiance observed by the detector is the same in all directions and is directly proportional to the cosine of the incidence angle. In this case, the BRDF is independent on both the direction of illumination and the direction of observation, and is equal to $1/\pi \text{ sr}^{-1}$.

The Lambert surface is only an ideal case and no known material displays perfect Lambertian behavior. However, the definition of the Lambert surface is necessary to define the “reflectance factor” that is widely used to characterize how surfaces scatter light.

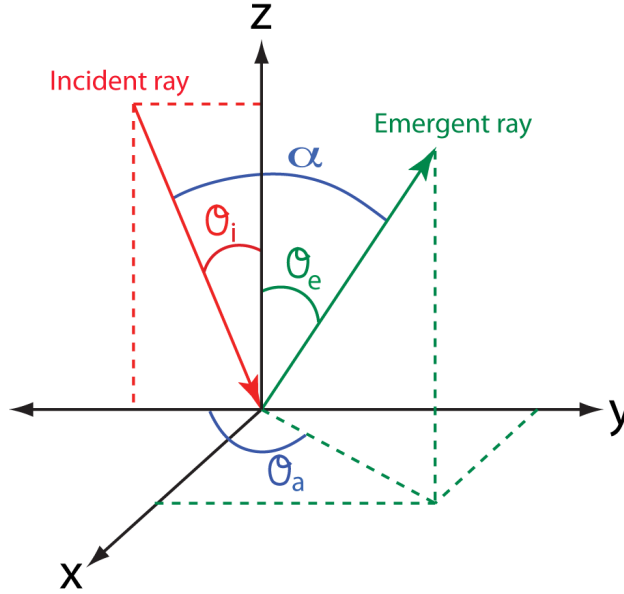


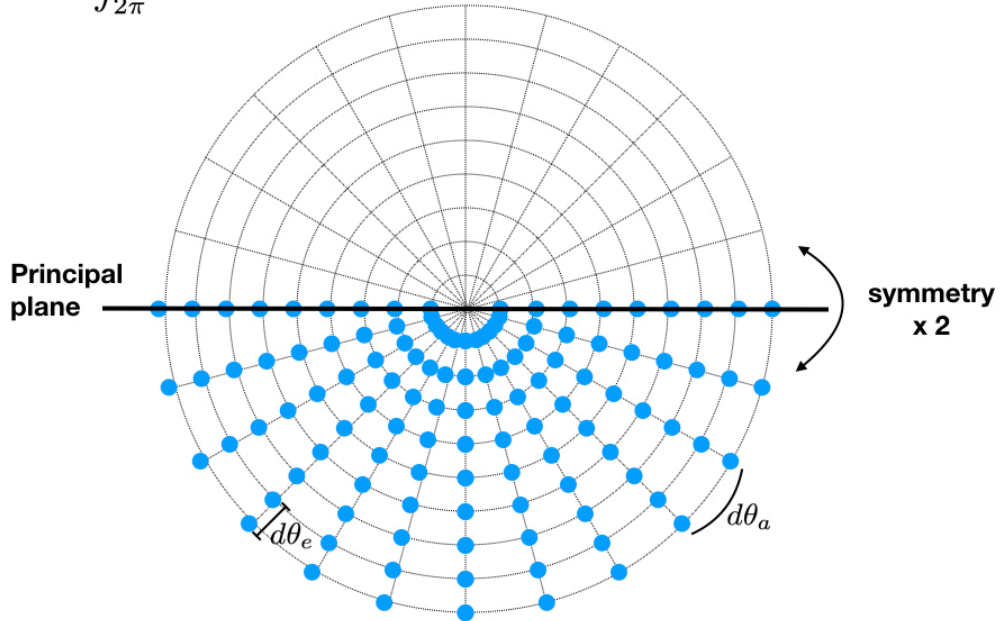
Figure 2: Definitions of the incidence (θ_i), emission (θ_e), azimuth (θ_a) and phase (α) angles. The measured surface is in the (x,y) plane. Incidence and emission angles are measured relative to the normal direction (z).

The reflectance factor, REFF, is defined as the radiance reflected by the surface in a given direction normalized to the radiance that would be reflected by a perfect Lambert surface illuminated and observed with the same geometry as the sample. Thus, the reflectance factor of a perfect Lambert surface is constant and equal to 1. As the ratio of two radiances, the reflectance factor is dimensionless. The relationship between the BRDF and the reflectance factor is straightforward: $REFF = BRDF \cdot \pi$. From this relation, we can also derive:

$$REFF_{\lambda} = \frac{\pi \cdot I}{F \cdot \cos \theta_i}$$

Another important photometric property that can be derived from the BRDF measurements is the directional hemispheric reflectance or directional albedo (hereafter: hemispheric reflectance R_H). It is defined as the ratio of all the energy reflected outward toward a semi-spherical hemisphere above the target surface to the incident energy onto the surface. It can be derived from BRDF measurements at a given incidence angle and a given wavelength by integration of the BRDF values over the emission and azimuth angles as illustrated in Figure 3.

$$R_H(\theta_i) = \int_{2\pi} BRDF(\theta_i) d\Omega_r \quad d\Omega_r = \cos(\theta_e) d\omega_r = \cos(\theta_e) \sin(\theta_e) d\theta_e d\theta_a$$



$$R_H(\theta_i) = 2 \int_{\theta_a=0}^{\theta_a=\pi} \int_{\theta_e=0}^{\theta_e=\frac{\pi}{2}} BRDF(\theta_i, \theta_e, \theta_a) \cos(\theta_e) \sin(\theta_e) d\theta_e d\theta_a$$

Figure 3: Illustration of the relation between the hemispheric reflectance R_H and the BRDF. The blue dots are the positions of the BRDF measurement points. Note the symmetry around the principal plane. Although the integration should in theory be performed for emission angle between 0 and 90°, it is in fact not possible to measure the BRDF at a phase angle of 0° and measurements at emission larger than 75° are affected by large uncertainty. Therefore, the points should be interpolated from neighbor points. Note however that because of the term $\cos(\theta_e) \sin(\theta_e)$ in the equation, values of BRDF measured at low and high emission angles do not contribute much to the final result.

3. Physics of the BRDF:

The BRDF of a surface is influenced by many parameters. The physics of the “radiative transfer” that governs the scattering of light by granular material is extremely complex, and constructing a complete model of these processes remains a challenge. In this section, we provide simple ideas on how the anisotropy of the BRDF is generated. For an extensive discussion of all these effects and how they are treated in a physical model, we strongly suggest referring to [Hapke \(2012\)](#), considered the main reference book on this topic.

We can distinguish two types of influences on the BRDF of planetary surfaces and their analog samples: microscopic and macroscopic. Microscopic effects are related to the intrinsic properties of the particles that compose the surface. Each particle of each material is characterized by intrinsic optical and physical properties that strongly affect the way it scatters light. These properties are described by the “optical constant”, which is a complex parameter that consists of a real part (also called refractive index) that describes how the material reflects light, and an imaginary part (also called absorption index) that describes how the material absorbs light. These indices affect the ratio between the amount of light that is reflected back in the incident direction and the amount of light that is transmitted through the grain, and thus have a strong influence on the BRDF. In addition, since both parts of the optical constant depend on wavelength, they provide the BRDF with some of its wavelength-dependence.

Beyond their intrinsic optical properties, the size and shape of the grains also strongly influence the BRDF. When the radius (R) of the grains changes, the ratio between their surface ($\sim R^2$) and their volume ($\sim R^3$) also changes, and with it the ratio between surficial (reflective) and volumetric (absorptive) effects. This gives rise to major variations in the shape of the BRDF. What happens when the size of the grains is of the same order as the wavelength of the incident light is still not completely understood, but it certainly contributes to the dependence on wavelength of the BRDF.

In addition to the effects at the scale of the individual grains, the way these grains are arranged together, and the macroscopic shape of the surface

also strongly affect the BRDF. In particular, the disappearance of shadows when phase angle decreases strongly contributes to the increase of reflectance at low phase angles, as seen for example, on the Moon ([figure 1](#)).

The BRDF is thus affected not only by the nature of the samples but also by their “texture”. Consequently, different surfaces prepared with the exact same materials but with different textures (for example: sprinkled vs. smooth) will result in very different shapes of the BRDF. This is an absolutely crucial point when measuring the BRDF of samples in the lab. BRDF measurements that are not accompanied by extensive documentation of the state of the measured surface (pictures, grain size distribution, microscopy, description of the preparation method) lose most of their scientific value.

4. The PHIRE-1 gonio-radiometer:

In this section, we briefly describe the different components of the PHIRE-1 gonio-radiometer. Detailed instructions on how to use this setup are provided as an appendix to this document.

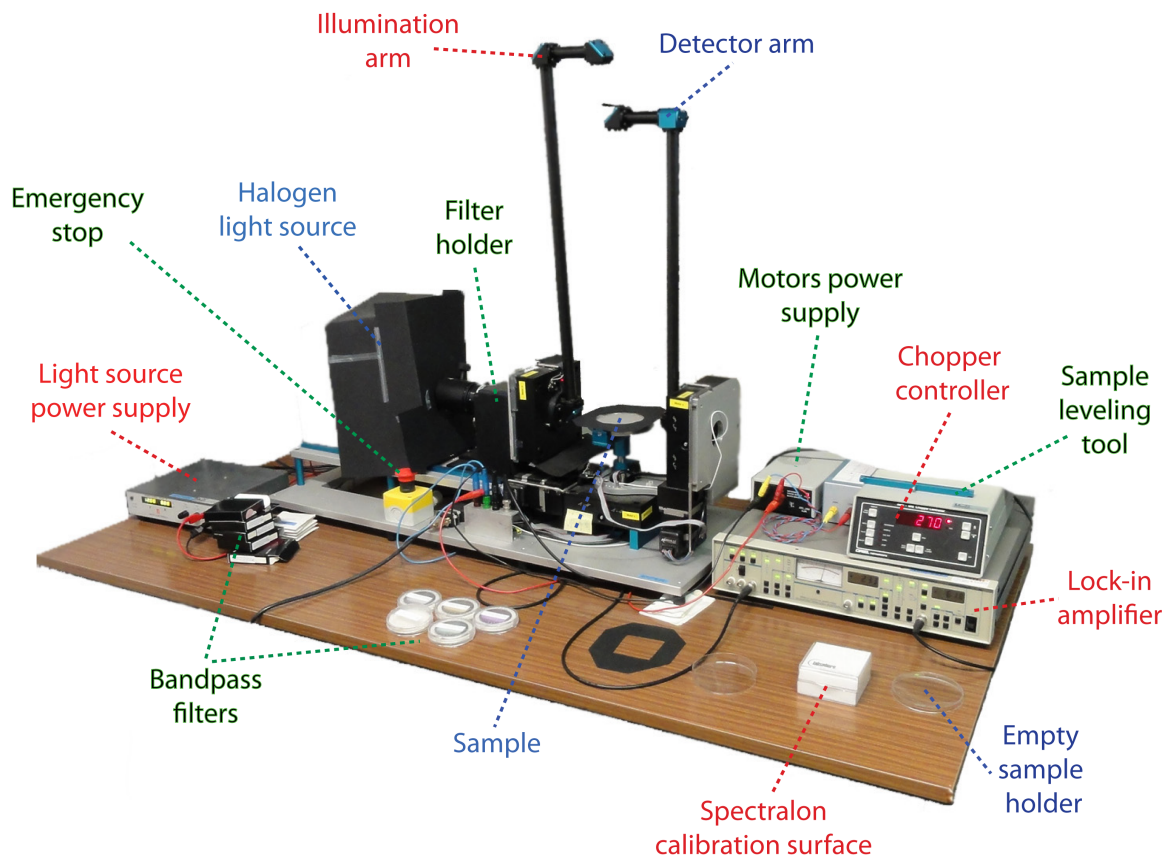


Figure 4: Picture of the PHIRE-1 gonio-radiometer with identification of the most important parts

Figure 4 shows the complete setup and identifies its different parts. The light source is composed of a halogen lamp in its enclosure and a power supply. As soon as it exits the source, a mechanical chopper (rotating wheel with apertures) modulates the light at high frequency. A chopper controller is used to define this frequency. Two-inch filters can then be introduced in the beam to select different portions of the visible and near-infrared spectrum, in narrow or wide bands. The light is then conducted through the illumination arm and projected onto a circular sample (typically 1 cm thick and 12 cm diameter). This illumination arm can be rotated on one side only, down to a maximum incidence

angle of 90° . When incidence angle increases, the length of the ellipsoidal light footprint onto the sample also increases proportionally to $\cos(\theta_i)$.

The light scattered by the sample is measured by a photodiode at the end of the detector arm. This detector arm can be rotated to any direction in a quarter of a sphere by moving on two axes: emission angle and azimuth angle (see [figure 2](#)). Note that the solid angle from which the detector receives light is always larger than the apparent angular extent of the illumination footprint. This facilitates the calibration of the measurements. All motors receive power from a single power supply and are remote-controlled from a computer.

The signal measured by the photodiode is analyzed by a “lock-in” amplifier that works together with the chopper controller. Lock-in amplification, or phase sensitive detection, is used to decrease the noise level created by ambient light by restricting the measurement of interest to a known frequency and filtering the retrieved signal inside a narrow band around this frequency. The resulting value of light flux retrieved by the lock-in amplifier is transmitted to the computer and stored in a text file for further analysis.

A few scripts and programs have already been written to automatically acquire a series of measurements, for example by moving the emission arm by steps of 5° between emission angles of -70° and $+70^\circ$, measure the reflectance at each step and store all data into a single file.

[Figure 5](#) presents examples of BRDF measurements acquired with the PHIRE-1 instrument. Two surfaces were prepared with the same basalt (common volcanic rock) powder sample. To prepare the first surface, the basalt powder was simply sprinkled into the sample holder. For the other, we pressed the surface slightly to make it perfectly smooth. Incidence angle was set at -60° and emergence angle was varied from -70° to $+70^\circ$ by steps of 5° . The same measurements were repeated with 5 different narrow bandpass filters. For both surfaces, we observe an increase of the reflectance at low phase angles (i.e. when emission/emergence angles gets closer to -60°), which is known as “back-scattering behavior”. In the case of the pressed surface we also observe a strong increase of the reflectance at high phase angles, which is known as

“forward-scattering behavior”. This example perfectly illustrates the importance of surface texture effects on the BRDF.

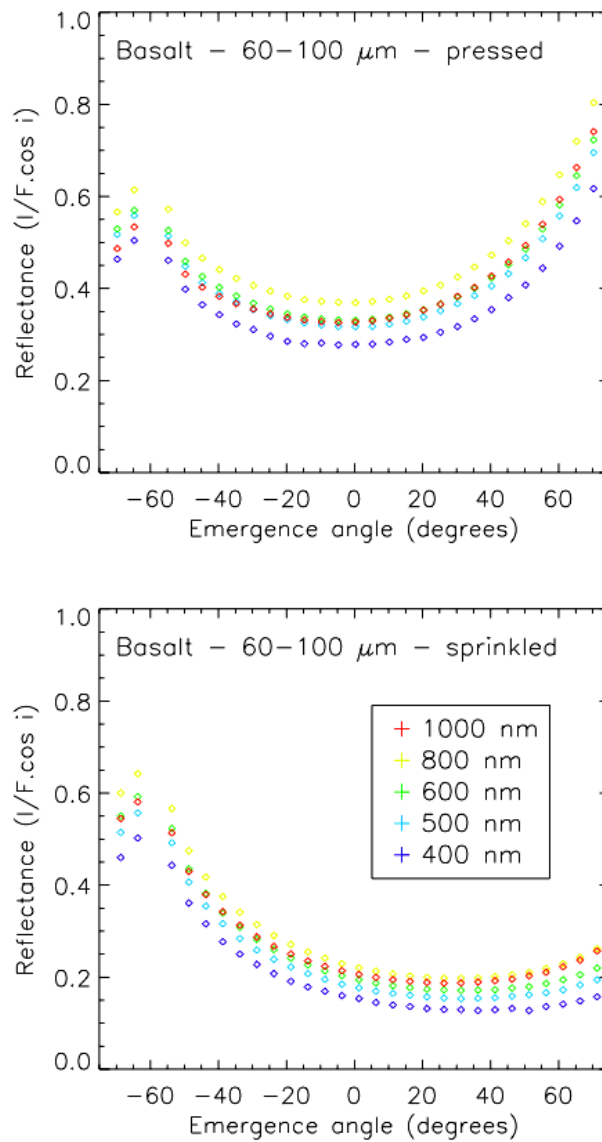


Figure 5: Example of BRDF measurements on the PHIRE-1 photo-goniometer.

5. Exercises:

** Before starting the exercises, make sure you have read Appendix A, that you are familiar with the experimental setup, and that you know how to calculate the BRDF from the voltage measurements and calibrate the instrument appropriately.*

5.1. Long-term Setup stability

Test the stability of the setup by measuring the signal from the reference target (spectralon) in a fixed geometry of your choice and with a given filter (e.g., Johnson-R) many times over the course of one to several hours (possibly overnight). During this sequence of measurements, turn the light of the room on and off of couple of times to see if this has an influence on the measured voltage. Don't forget to note the time when you start your measurements. Plot the results: First plot the signal in volts as a function of time in hours, then calculate the Reflectance Factor (REFF) using the Calibration Constant and plot it as a function of time in hours. Compute the average and standard deviation of the signal and discuss your observations.

5.2. Reciprocity principle

Test the reciprocity principle by measuring the reflectance of the reference surface (Spectralon) in pairs of configurations in which the incidence and emission directions are swapped. Use the Johnson-R filter and restrict these measurements to the principal plane. Calibrate the results and calculate the relative difference for each pair of configurations. Compare these values to the standard deviations obtained in 5.1 and discuss the results. Compute the median of the series of relative differences. This median value can later be used as an uncertainty or error bar on your measurements.

5.3. Diffuse and specular black surfaces on the principal plane

In the principal plane, measure the reflectance of two samples of the Acktar[®] material ("metal velvet" and "spectral black"), for emission angles varying from -75° to 75° , and three incidence angles (0 , 30 , and 60°). Use the Johnson-I and

Johnson-V filters. Compare the calibrated reflectance curves for each band and discuss the results.

5.4. Surface of a CD/DVD on the principal plane

In the principal plane, measure the reflectance of the surface of a CD or DVD for emission angles varying from -75° to 75° and three incidence angles (0 , 30 , and 60°). Perform the measurements with different wavelength filters (at least three). Compare the calibrated reflectance curves for each band and discuss the results.

5.5. Roughness of a sand sample on the principal plane

Prepare a surface made from sand and measure its reflectance. Using the same material, first prepare a smooth surface and measure its reflectance at one wavelength in the principal plane. Perform measurements over a wide range of emission angles and for a few incidence angles. Then, alter the state of the surface by creating patterns: pits, troughs, etc. and repeat the measurements. Make sure the scale of the patterns you apply to the surface remains small compared to the spot size of the illumination beam.

5.3. Hemispheric reflectance of the Spectralon

Measure the reflectance of the Spectralon at varying emission (0 - 75° by steps of 5°) and azimuth angles (0 - 180° by steps of 15°), for three different incidence angles: 0° , 30° and 60° . **Be extremely careful when varying the azimuth angle, as there is a risk of collision if the angles are not correctly selected (See Appendix A).** Perform all measurements with the Johnson-R filter. Plot the reflectance values in the principal plane (azimuth = 0 or 180°) as 2D plots (i.e., reflectance factor as a function of emission angle for the three incidence angles). Try to plot all values, including those out of the principal plane, using a projection in spherical coordinates (orthographic or equidistant). See example in [Fig. 3](#). Perform the integration of the BRDF values to calculate the hemispherical reflectance at the three different incidence angles. To do so, you can extrapolate the values at high emission angles by setting $REFF=0$ for $e=90^\circ$

and interpolating linearly in between the maximum measured emission angle and 90°. Interpolate the value of REFF at 0°-phase angle from REFF values at 5°. Discuss the values you obtain. Reminder: the manufacturer guarantees a hemispherical reflectance of 0.99 for this sample.

5.7. Optional: Propose your own idea for a measurement

Bring a sample, measure its reflectance, calibrate the data and discuss the objectives of your measurements and results.

References:

Gunderson, K., Thomas, N., and Whitby, J. A., First measurements with the Physikalisches Institut Radiometric Experiment (PHIRE), *Planetary and Space Science*, **54**, p. 1046-1056, 2006.

Gunderson, K., Lüthi, B., Russell, P., and Thomas, N., Visible/NIR photometric signatures of liquid water in Martian regolith simulant, *Planetary and Space Science*, **55**, p. 1272-1282, 2007.

Gunderson, K., and Thomas, N., Polarimetric NIR reflectance measurements of regolith simulants at zero phase angle, *Planetary and Space Science*, **56**, p. 1925-1938, 2008.

Hapke, B., Theory of Reflectance and Emittance Spectroscopy, Second Edition, *Cambridge University Press*, 2012.

Lüthi, B., PhD Thesis, *Physikalisches Institut – Universität Bern*, 2009.

Schkuratov, Y., and Kreslavski, M., A model of Lunar photometric function, *29th LPSC conference*, abstract # **1117**, Houston, Tx, 1998.

Shkuratov, Y., Starukhina, L., Hoffmann, H., and Arnold, G., A model of spectral albedo of particulate surfaces: implications for optical properties of the Moon, *Icarus*, **137**, p. 235-246, 1999.

Appendix A (detailed user manual):

** Turn on the “lock-in” amplifier first.*

[1] Light source:



Light is provided to the setup by a 100 W halogen lamp. To preserve this lamp, it is important to always apply smooth and slow changes of voltage and current.

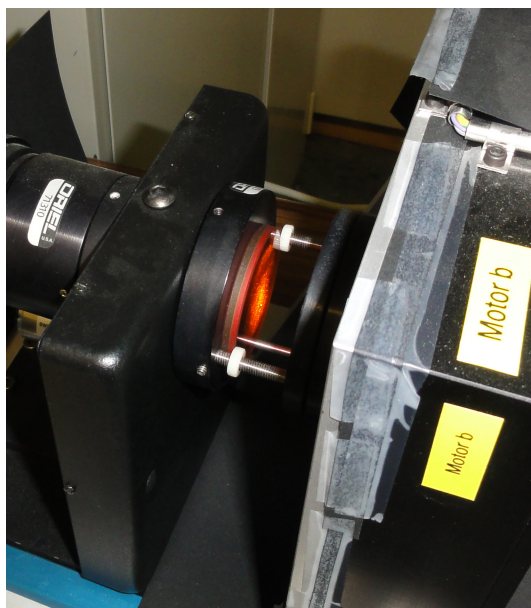
Please follow these procedures:

- To turn the lamp on: as the power supply is switched off, turn the voltage hand knob (“CV”) left to the lowest value and turn the current hand knob (“CC”) right to the highest value. Then, switch on the power supply and slowly increase the voltage up to **10 Volts**. The current value should be **just above 8 A**.
- To turn the lamp off: slowly decrease the voltage down to 0. Then, switch off the power supply.

[2] Motor power supply:

Simply switch this unit on or off (the switch is located on the rear panel). After turning the unit on, you have to run the motor_init script to initialize the 0 position of each motor (see section 8 of this user manual).

[3] Filter holder:



Remove the black metallic protection over the filter holder. Put the filter in place and secure its position by screwing the two white disks. Do not touch the surface of the filter with your fingers (use powder-free gloves). Put back the protection.

[4] Chopper:



Switch on the unit (the switch is located on the rear panel). Start the chopper by pushing the “RUN” button. Then, wait until you read the frequency on the display. To turn the chopper off, push either the “STOP OPEN” or “STOP CLOSED” button.

You can change the chopper frequency by using the “UP” and “DOWN” keys in the right part of the front panel. Once you have obtained the desired

frequency, push the “SET” key to immediately apply the new setting. The lock-in amplifier will then automatically synchronize to the chopper.

A good setting for the chopper frequency is 70 Hz. Other values can also work. Feel free to experiment that yourself and change the chopper frequency to see its effect on the signal/noise ratio of your measurements.

[4] Lock-in amplifier:

***Turn this on first**



The most important parameters that you will have to set are the *sensitivity* and the *time constant* (this latter parameter can usually be set from the computer). Other parameters can be set to default values as shown on the picture. To learn more about the lock-in amplification technique, directly refer to the user manual of the lock-in amplifier where the meaning and influence of all parameters are extensively described. You can test the effects of the different parameters by repetitively acquiring series of measurements and varying some settings.

Time constant: This parameter has a strong influence on the signal/noise ratio and on the response time of the instrument. With a high time constant, you will get a better signal/noise ratio but the system will respond slower to a change in the measured light flux. With a lower time constant, the signal/noise ratio will be degraded but the system will react faster. The standard way of operating the lock-in amplifier is the following: prior to any change in the configuration (change in the position of the arms, filter, sensitivity), we lower the time constant to 0.3 s. Once the new configuration is reached we progressively increase the time constant, step by step, and at each step we wait for the duration of one time constant (0.3 s at time constant=0.3, 1 s at time constant = 1, 3 s at time constant = 3...) until the desired time constant is reached. Then, we let the system stabilize for the duration of two time constants and acquire a

measurement. Normally, we use a time constant of either 3 or 10 s, depending on the reflectance of the sample and the filter used. This procedure is already implemented in the computer programs that we use to control the instrument.

In addition to the main sensitivity setting, you might also find useful to change the “DYN RES” (dynamic reserve) setting. Normally, this should be set to “NORM”. However, if the signal is very low, it might be necessary to switch to “HIGH” dynamic reserve. Because, it is not straightforward to determine which setting is better, you are encouraged to make tests to determine which one is the most appropriate for your measurements.

Sensitivity: you have to manually select a sensitivity range that you will use for the entire set of programmed measurements. The sensitivity range should be the lowest possible value (highest sensitivity) so that you don't overload the detection system. Use the two keys at the bottom of the sensitivity range panel to change the range. Check the “OVLD” LED in the status panel (right of the sensitivity panel). This LED will turn red and blink if overload is detected. In that case, set the sensitivity to a higher range. Use a short time constant (0.3 or 1 s) when selecting the most appropriate sensitivity range so that you get faster responses of the system. The sensitivity setting will be used for a complete set of measurements. Therefore, you have to adjust this setting for the position where you expect the maximum of light to reach the detector. This will always append when $\theta_e=0^\circ$ (vertical detector arm) because the amount of light that reach the detector is proportional to $\cos(\theta_e)$. If the sample displays a predominant back-scattering behavior, the maximum will occur at low phase angle and you should set θ_i to 5° . If the sample displays a predominant forward-scattering behavior, the maximum will occur at high phase angle and you should set θ_i to about 70° . If you are not sure about the scattering behavior of the sample, check these two positions.

[6] Sample preparation and installation on the instrument:

We use plastic Petri dishes to prepare the samples. Fill one of these dishes to rim with the sample powder. Then, different methods can be used to

prepare/alter the surface state (see discussions in various sections of this document).

Once the sample is ready, install it in the sample holder on the goniometer. Use the black paper masks to avoid stray light reflections on the sample holder (see [figure 4](#)). You will have to level the sample holder so that the surface of the sample is in the same plane as the rotation axes of the two arms. To do so, use the sample leveling tool (the blue aluminum bar with a steel pin in the middle, see [figure 4](#)). Insert it between the basements of the two arms when both are in 0 position. Then, carefully unscrew the sample holder on its vertical axis (the screw is located below the sample holder), move the sample holder vertically until the extremity of the pin touches the surface of the sample and secure this position by locking the screw.

[7] Calibration of the BRDF measurements:

The photodiode / lock-in amplifier returns voltage values that have to be converted to reflectance values. To do so, we normalize the voltage values obtained with the sample by voltage values obtained with a reference surface whose scattering behavior is relatively close to the one of a perfect Lambert surface (see [section 2](#)). As a reference, we use the Labsphere Spectralon™ surface. We have determined that the bidirectional reflectance factor of this reference surface is equal to its hemispherical albedo, $A_H=0.99$, when: $\theta_i = 0^\circ$, $\theta_e = 55^\circ$ and $\theta_a = 0^\circ$. We use this property to calibrate the measurements of the sample:

$$C_\lambda = \frac{A_H \cos(55^\circ)}{\pi \cos(0^\circ)(V_{ref} - V_0)}$$

$$BRDF_\lambda = C_\lambda \frac{(V_{sample} - V_0)}{\cos\theta_e}$$

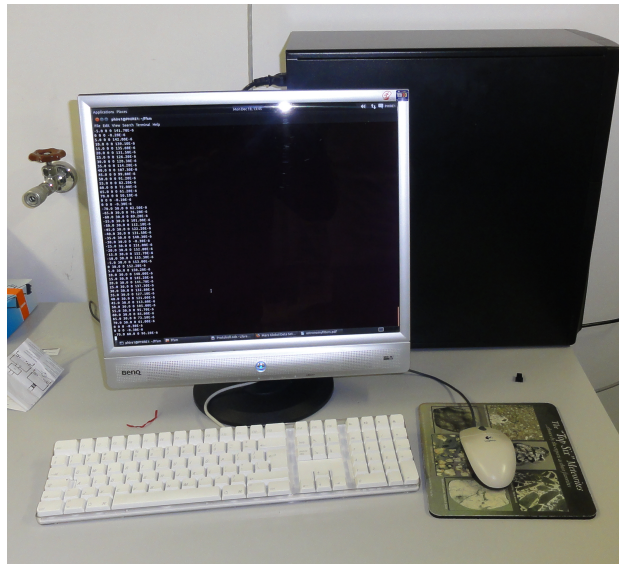
$$R_\lambda = \pi \cdot BRDF_\lambda$$

First, we calculate the calibration constant C (that is actually dependent on the wavelength, i.e. you have to measure/calculate it for each different filter) from a measurement of the Spectralon reference surface with the particular geometry already described. The constant calculated from this measurement

can then be used to calibrate the BRDF or Reflectance Factor values for the sample (using the same filter).

Note that in these equations, we always take into account a possible voltage offset V_0 that is measured before and/or after the measurement on the sample when $\theta_i=\theta_e=\theta_a=0^\circ$. In this particular position, the extremity of the detector arm completely masks the incident light beam and no light reaches the sample (“dark voltage measurement”). Script # 4 in run_phire.py will automatically perform the measurement under the appropriate geometry as well as the dark voltage measurement.

[8] Computer control:



Series of measurements can be programmed from the computer and all data can be saved to simple text files that can then be opened from any software. The computer control system, originally consisting of compiled C programs and bash scripts running on a Linux computer, has been entirely re-implemented as Python interactive scripts. Currently, we are using the Spyder python compiler to operate the experimental setup and program the measurements. The original structure and content of the procedures and functions has been maintained so that the new programs should work exactly as the original ones and give the same results. See Appendix B for examples of procedures and directly use

them to acquire standard series of measurements or customize them to build your own acquisition sequences.

Default Login / Password: Student / phire2015stud (TBC)

Ask the assistant in case this doesn't work. The login information might have been changed for various reasons.

Start the Spyder python editor. You can now open the various scripts, run them independently, combine them and modify them according to your needs.

[9] Emergency Stop Button and Reset

The big red button on a yellow base next to the light source is the 'Emergency Stop' button. It is meant to cut power to the experiment and stop the arms from continuing to move if there is an imminent collision. **Only use it if you see that the arms will collide with each other or with something else if they continue on their current trajectory.** If you have read this script and done the experiment correctly and carefully, familiarizing yourself with the movement of the arms before attempting to move the azimuth angle, **there is no reason why you should have to use this button.**

If however, you made a mistake and you see the arms are about to collide, you will need to use it to prevent the instrument from breaking. If you do use it, you will need to reset the setup:

- (1) First make sure that after you have pressed the button, you turn and release the button to its initial position.
- (2) In the phire_python_prog folder in the desktop, find the motor_pos text file and change the values to the approximate current angular positions of the arms, after the experiment was stopped. In that file, the first line is the angle for Motor a (emission), the second line is the angle for Motor b (incidence), and the third line is the angle for Motor c (azimuth). Try to match the angles as closely as you can to the arm positions.
- (3) Test that you got the motor_pos angles correctly with the move_and_wait command. Move the arms only slightly (2-5 degrees)

AWAY from each other to make sure that you got the angles correctly and won't cause another collision.

- (4) Send the arms back to their home position by initializing the motors, using the `motor_init()` command.

[10] Specific Commands:

motor_init()

This command will initialize the position of the motors. It has to be executed after you turn on the motors power supply prior to any other action.

move_and_wait(e,i,a)

This command accepts three arguments: emergence angle, incidence angle and azimuth angle respectively (separated by commas). For example:

```
move_and_wait(30,-60,0)
```

will result in movements of the illumination and detector arms until the incidence angle is -60° and the emergence angle is 30° . In that case, there is no movement in azimuth.

Be extremely careful with this command if you specify a change in the azimuth angle. In that case, there might be a risk of collision of the arms. Proceed carefully by small steps. Or even safer: always go back to (0,0,0) between two measurement positions when the azimuth is changed (of course this takes more time).

move_and_measure(e,i,a,time_const,sleep_time,file)

Accepts the three angles first (as `move_and_wait`) then a time constant and a sleep time for the lock-in amplifier and finally a filename to store the measure. For example:

```
move_and_measure(30,-60,0,3,6,'my_data_file.dat')
```

Be extremely careful with this command if you specify a change in the azimuth angle. In that case, there might be a risk of collision of the arms. Proceed carefully by small steps.

You can easily write your own scripts to acquire customized series of measurements. As a starting point, in the `run_phire.py` program, copy and

paste script # 1 to the uncommented section at the top of the file and change the emission and incidence angles and see how this procedure makes use of the move_and_wait script. If you want to write a script that modifies the azimuth angle you must be VERY careful, since if this is done incorrectly, there is a risk of the arms colliding. **DO NOT change the azimuth angles until you are very familiar with the movement of the arms and the experimental setup.** If you want to do it, first check the different positions step by step. We strongly recommend that you move both arms to 0 position before applying any change in the azimuth angle.